C. R. Geoscience 342 (2010) 483–491

Contents lists available at ScienceDirect

Comptes Rendus Geoscience

www.sciencedirect.com

Geodynamics

Diagenetic signature of the Mid-Paleocene exposure surface in the southeastern Pyrenean platform

Signature diagénétique de l'émersion du Paléocène moyen au sud-est de la plate-forme pyrénéenne

Eloïse Kiefer-Ollier *, Corinne Loisy, Adrian Cerepi

EA no. 4134 GHYMAC, institut EGID, University of Bordeaux, 1, allée Daguin, 33607 Pessac, France

ARTICLE INFO

Article history:
Received 29 August 2008
Accepted after revision 11 January 2010

Presented by Jean Aubouin

Keywords:
Diagenesis
Subaerial exposure
Vadose zone
Paleocene
South-Pyrenean basin
Campo section

Mots clés :
Diagenèse
Émersion
Zone vadose
Paléocène
Bassin sud-pyrennéen
Coupe de Campo

ABSTRACT

From Danian to Thanetian, the South-Pyrenean carbonate platform underwent the most important Paleocene marine level fall of approximately 60 m magnitude. The palaeoenvironmental setting related to the highstand systems tract was defined thanks to detailed petrographical descriptions of the sedimentary facies. These conditions are based on a "hypersaline lagoon and prograding subtidal sabhka" model. The descriptions of diagenetical processes show that the lowstand period is underlined by the following six major diagenetic stages: early processes related to depositional environment, meteoric karstification, meteoric cementation, mixed corrosion and precipitation, and burial. We propose this sequence such as the diagenetic signature of the Mid-Paleocene subaerial exposure.

RÉSUMÉ

Les dépôts sédimentaires paléocènes de la plate-forme carbonatée sud-pyrénéenne ont enregistré une chute du niveau marin d'une amplitude minimum de 60 m entre le Danien et le Thanétien. Une étude pétrographique détaillée des faciès sédimentaires situés sous la limite de séquence permet de définir le contexte environnemental à la fin du prisme de haut niveau basé sur un modèle de type « lagon hypersalin et sabhka subtidale progradante ». La description des processus diagénétiques montre que la période de bas niveau marin est marquée par les six phases diagénétiques majeures suivantes : processus précoces liés à l'environnement de dépôt, karstification en zone météorique, cimentation en zone météorique, corrosion et précipitation en zone mixte, et enfouissement. Cette séquence est proposée comme signature diagénétique de l'émersion du Paléocène moyen.

1. Introduction

Aguirre et al., 2007 and Baceta et al., 2005 have noticed that 28 physical and biotic events, including subaerial exposure and flooding stages caused by marine fluctuations, were recorded in the south-eastern Paleocene Pyrenean shallow marine carbonated platform. The synthesis of all these events shows that the most important changes take place around the NP4-NP5 boundary (Martini, 1970), during a regionally extended level fall expressed by an unconformity surface on the platform top: the Mid-Paleocene Unconformity (MPU). The

* Corresponding author.
E-mail address: eloise.kiefer@egid.u-bordeaux3.fr (E. Kiefer-Ollier).

1631-0713/$ – see front matter
doi:10.1016/j.crte.2010.02.006

aim of this article is to define the diagenetic sequence that characterized the Mid-Paleocene exposure surface in the South-East of the Pyrenean platform. The studied transect, presented on Fig. 1A is composed of three Paleocene stratigraphic sections limited by the Esera river and the Merli village (Aragon, Spain): Campo, Feixa-Rasa and Merli. The results allow us to propose new conceptual models integrating paleoclimatic, paleohydrogeologic and environmental conditions during the Late Danian low-stand marine period. In the global context, this study participates in recent scientific research about climate evolution during the Early Paleogene (Pujalte et al., 2006).

2. Geological setting

The Paleocene period of the Pyrenean surrection started with the collision between Iberian and European plates (Muñoz, 1992). From Cretaceous to Paleogene, a single westward opened basin is developed in the present location of the Pyrenees (Fig. 1B). Before its enclosure, the Eocene-Oligocene east-west propagation of the Pyrenean orogen (ECORS-team, 1989) generates the distinction of two foreland basins (Ardèvol et al., 2000): the Aquitanian basin on the north and Ebro basin on the south. At the same time, the southern part is affected by a large overlapping and the individualization of three sedimentary sub-basins: Pamplona, Jaca and Graus-Tremp (Payros et al., 1999). The study area is located in the Graus-Tremp foreland basin, developed in piggy-back thanks to Montsec and Cotiella overlaps (Casas et al., 2002) (Fig. 1A). According to Casas et al., 2002 and McClay et al., 2004, the internal structure of the Cotiella unit is dominated by Turonian extensive kilometer scale tectonic structures. These structures are probably reactivated during the Late Cretaceous to Paleocene, after the alpine compressive stage. New bio-chronostratigraphy (Bernaola, 2002; Orue-Etxebarria et al., 2001; Pujalte et al., 2003), cyclo and magnetostratigraphy (Dinarès-Turell et al., 2002; Dinarès-Turell et al., 2003; López-Martínez et al., in press; Pujalte et al., 1995), and isotopic (Schmitz and Pujalte, 2003) data were recently obtained on Maastrichtian-Ilerdian sedimentary series. These results allow Baceta et al., 2004 and Robador, 2005 to define six eustatic cycles of third order (Vail et al., 1977) in the whole South-Pyrenean platform and particularly in the Campo area: SD-Da/Ma, SD-Da1, SD-Da2, SD-Th1, SD-Th2 and SD-Il1 (Fig. 1C). The palaeogeographical setting during the Danian (Baceta et al., 2005) locates the study area in a transition domain between shallow marine carbonated platform and lacustrian-paludal continental system (Fig. 1B). Because of the geographical situation, minor and major sea level oscillations were recorded in the depositional series. The third order sequence boundaries are subaerial exposure surfaces marked by more or less high continental degrees. The boundary between SD-Da2 and SD-Th1, called Mid Paleocene Unconformity (MPU) is the most important (Fig. 1C). The associated sea level fall is estimated between 80 to 100 m in the South-West of the basin by (Baceta et al., 2007). During the lowstanding period, the top of the platform is entirely subaerially exposed with a development of specific markers like

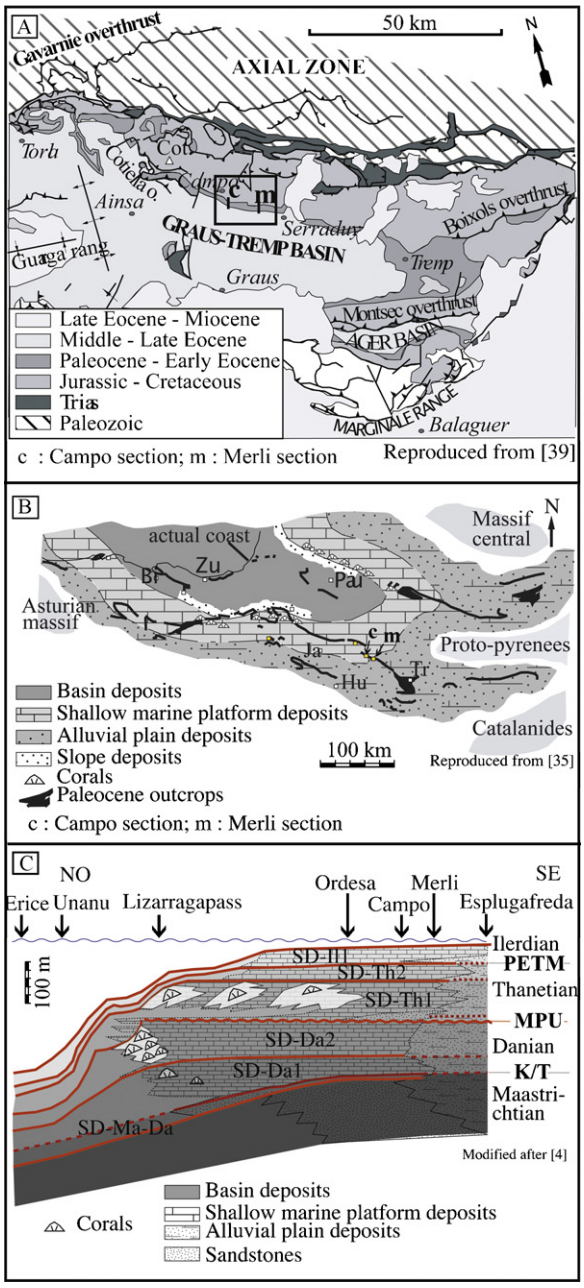

Fig. 1. (A) Geological and structural map of the Graus-Tremp basin (South-Pyrenean) (Robador, 2005). (B) Paleogeographic sketch of the Pyrenean carbonated platform during the Early Paleocene (Pujalte et al., 2006) and location of the study area (framed). Abbreviations: Zu: Zumaia, Bi: Bilbao, Hu: Huesca, Ja: Jaca, C: Campo, Tr: Tremp. (C) Sedimentary and stratigraphical setting of Paleocene platform, modified after (Baceta et al., 2004).

Fig. 1. (A) Carte géologique et structurale simplifiée du bassin de Graus-Tremp (Sud-Pyrénéen) (Robador, 2005). (B) Schéma paléogéographique de la plate-forme carbonatée pyrénéenne au Paléocène inférieur (Pujalte et al., 2006) et localisation de la zone d'étude (encadré). Abréviations : Zu : Zumaia, Bi : Bilbao, Hu : Huesca, Ja : Jaca, C : Campo, Tr : Tremp. (C) Contexte sédimentaire et stratigraphique de la plate-forme Paléocène, modifié d'après (Baceta et al., 2004).

karstic caves and pedogenesis. The Danian slope is dug by erosional scarps and depressions filled by breccias (Robador, 2005).

3. Material and methods

Succeeding field campaigns allow us to study the Paleocene outcrop sections of Campo (Toullec, 2006) and Merli, respectively 300 and 100 m of thickness. Eighty-one samples were taken under and above the Mid-Paleocene Unconformity (MPU). The samples were petrographically studied in non-covered and polished thin sections. Clasts and binders were described and counted in order to determine the sedimentary facies, using the Dunham classification (Dunham, 1962). Diagenetic transformations were petrographically identified and sorted out using Purser (Purser, 1980) and Moore (Moore, 2001) nomenclatures. The classifications of Choquette and Pray (Choquette and Pray, 1970) and Lucia (Lucia, 1995) were used to characterize the porous space. Dolomite morphologies have already been classified by Sibbley and Gregg (Sibley and Gregg, 1987) and Gregg and Sibley (Gregg and Sibley, 1984). Complementary analyses were realized with the cathodoluminescence and the Scanning Electron Microprobe (SEM) techniques. For each sample, diagenetic features were identified and chronologically arranged in order to deduce the major diagenetic sequence associated to the MPU.

4. Danian sedimentary facies and depositional environments

Five main groups of sedimentary facies were petrographically identified in thin sections. Their distribution in an Early Paleocene platform conceptual model is proposed in Fig. 2. Its building is based on the model of (Lindsay, in press) and is described in more details by Kiefer-Ollier, 2009.

4.1. Paludal limestones (GF-a)

Description: This group of facies (Fig. 3D–G) is represented by limestones composed of Microcodium colonies, abiotic mudstones enriched in organic matter and affected by subvertical oxidation traces, and alluvial silts affected by some ferruginous and carbonated segregations.

Interpretation: Microcodium, subvertical oxydations and nodular concretions are similar to roots (Bignot, 1994) formed in pseudogley hydromorphous paleosoils made only if the soil water-block is temporary, generally due to seasonal variations (Plaziat, 1984). The depositional environment associated to this group of facies is marsh of lacustrine coast or alluvial plain liable to periodical flooding.

4.2. Lacustrine limestones (GF-b)

Description: The GF-b group contains two types of limestone facies: abiotic mudstone with bird's eyes, and mudstone-wackestone with "charophytes", remains of ostracod and Microcodium, gastropods and little quartz grains (Fig. 3D).

Interpretation: According to fossil constituents, the depositional environment is interpreted as a shallow subaquatic depositional environment with a good oxygenation, luminosity and freshwater. The absence of subaerial features allows to distinguish this lacustrine facies from paludal GF-a.

4.3. Lagoonal limestones (GF-c)

Description: The group of facies GF-c includes biomicritic limestones containing charophytes, ostracods, discocyclines or miliolids (Fig. 3E). Some grains of quartz could be found.

Interpretation: The association of freshwater and salt-like organisms which characterizes subaquatic environments undergoes temporal and spatial salinity changes.

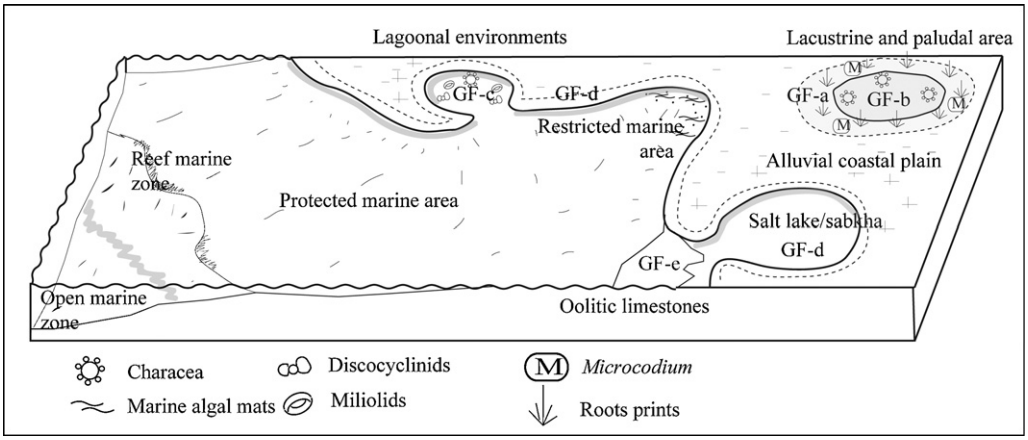

Fig. 2. Conceptual sketch of the distribution of the depositional environments and associated facies in the Early Paleocene platform. This sketch was inspired by the Lindsay model (Lindsay, in press). See the text for details about designation and description of the main group of facies (GF).

Fig. 2. Schéma conceptuel de la répartition des environnements de dépôts et des faciès qui leur sont associés sur la plate-forme au Paléocène inférieur. Ce schéma a été élaboré à partir du modèle de Lindsay (Lindsay, in press). L'appellation et la description des groupes de faciès (GF) sont détaillées dans le texte.

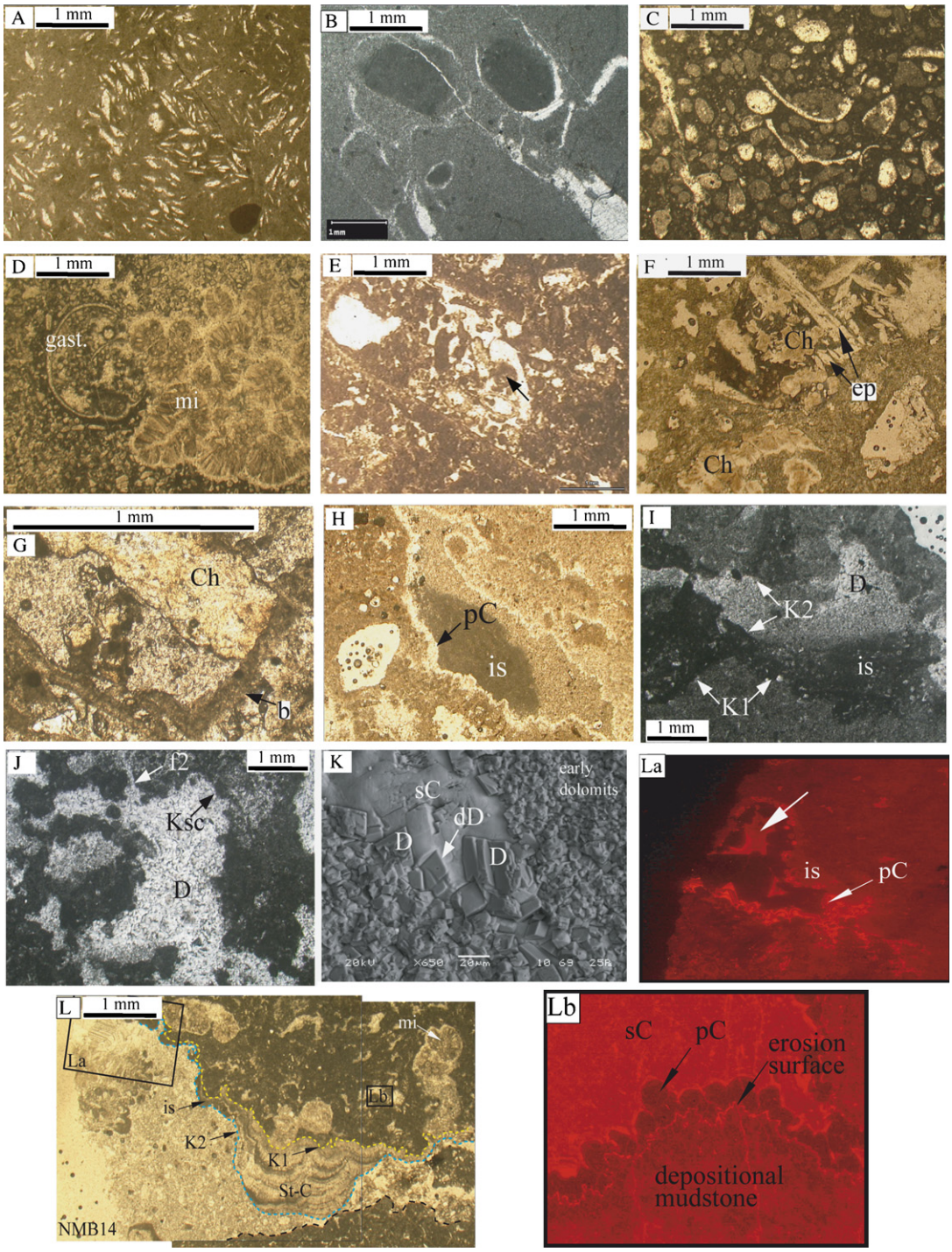

Fig. 3. Pictures of thin sections analyzed with optical microprobe (A to L) and cathodoluminescent technics (La and Lb) illustrating the different group of sedimentary facies and the main diagenetical process of subaerial exposure. A more detailed description of the pictures is given in this article. Signification of the abbreviations: gast: gastropods, mi: Microcodium, Ch: chalcedony, ep: evaporite pseudomorph, pC: dog-tooth calcite cements, is: internal sediment, K1: first stage of karstification, K2 or Ksc: second stage of karstification called "swiss-cheese", D: dolomite, dD: dedolomitization, St-C: stalactitic cement.

Fig. 3. Photographies de lames minces analysées au microscope optique (A à L) et en cathodoluminescence (La et Lb) illustrant les différents groupes de faciès sédimentaires et les principaux processus diagénétiques associés à l'émersion du Paléocène moyen. La description détaillée des photographies est donnée dans le texte associé. Signification des abréviations : gast : gastéropodes, mi : microcodiums, Ch : calcédoine, ep : pseudomorphoses d'évaporites, pC : ciment de calcite en dent de chien, is : sédiment interne, K1 : première phase de karstification, K2 ou Ksc : deuxième phase de karstification dite « swiss-cheese », D : dolomite, dD : dédolomitisation, St-C : calcite stalactitique.

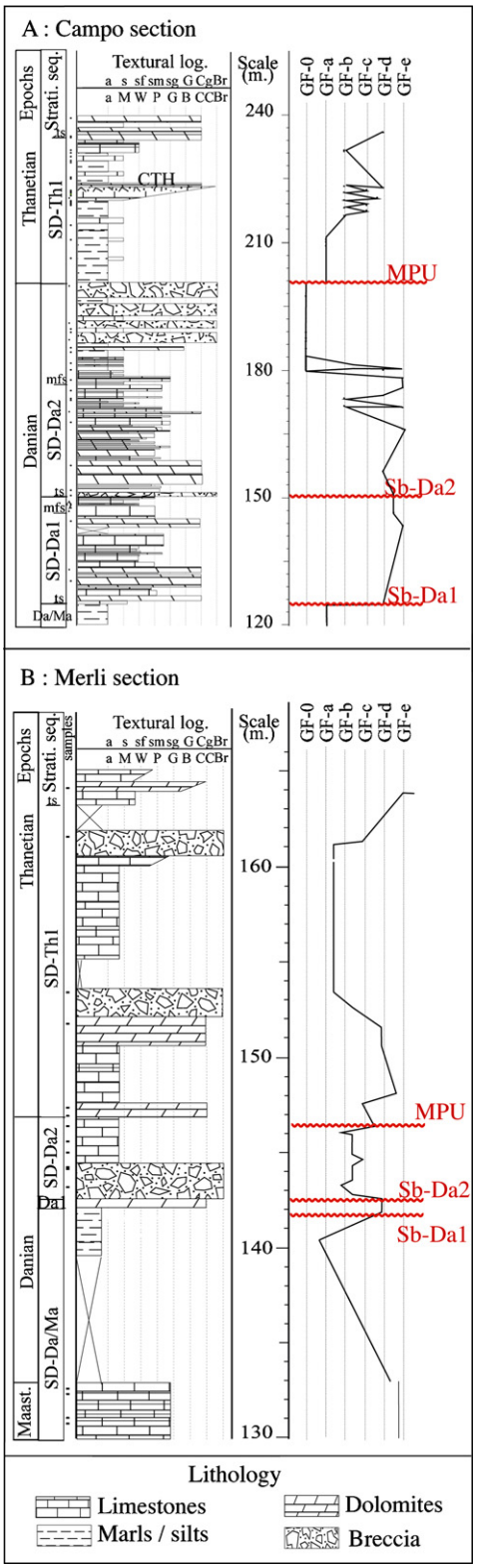

Fig. 4. Stratigraphical and textural profile of Campo (A) and Merli (B) sections, and evolution of the main groups of facies identified by petrographical analyses of each sample.

The depositional environment could be interpreted like a lagoon or a marine waters area isolated from open marine sea by subaerial lands. The changes of salinity could be induced by variations of evaporation, water depth, ocean water supply due to marine level variations, and fresh water supply of fluvial, meteoric or phreatic origin.

4.4. Evaporitic limestones (GF-d)

Description: The group of facies GF-d is composed of mudstones with lenticular evaporitic crystals pseudomorph (gypsum) (Fig. 3) replaced, during diagenesis, by chalcedony or amorphous silica, and microcrystalline limestone or dolostone (microdolomites) with syneresis cracks (Fig. 3A–B).

Interpretation: Mudstone with gypsum is deposited in a quiet and shallow subaquatical environment exposed to high evaporation rate and over saltness. It could be a salt lake-like sabkha system or an evaporitic lagoon underdrained by marine water. The syneresis cracks are related to shallow subaquatic environments affected by periodical immersion and emersion. Crystallization of microdolomites shows that a process of evaporation is dominating.

4.5. Oolitic limestones (GF-e)

Description: This facies is formed by an accumulation of small ovoid ooids (diameter: 340 μm max) (Fig. 3C). The ooids in which the cortex presents concentric structures seem to be ancient micritized ooliths. Other ooids are associated to altered benthic foraminiferal and endoclasts. The binding phase is composed of a dark micritic matrix.

Interpretation: The interpretation of the depositional environment of this ooids is difficult. The association with benthic foraminifers indicates a marine origin; the presence of mud in the interparticular porous network indicates a shallow and very calm depositional environment. Micritization is due to bacterial activity, generally in closed systems. According to (Da Silva et al., 2009; Flügel, 2004; Purser, 1980), these ooids are formed in subtidal marine protected area with low water energy environment and periodically affected by storms which accumulate the ooids in sandbars.

5. Sedimentary description of the studied sections

The studied transect composed of three Paleocene sections (Campo, Feixa-Rasa and Merli) allowed us to identify a sedimentary facies succession that reflects the sea level variations during the Early to Middle Paleocene. The results are given on Fig. 4. The sedimentary facies succession during the Early to Middle Paleocene reflects the sea level variations.

Fig. 4. Profil stratigraphique en texture des coupes de Campo (A) et de Merli (B) et évolution des groupes de faciès (GF) identifiés par analyse pétrographique d'échantillons.

5.1. Campo section

In the Campo section presented on Fig. 4A, the Da-2 sequence boundary is an erosional subaquatic surface characterized by reworked facies which contain marine and terrestrial bioclasts like red algae and Microcodium. The transgressive sequence (25 m) is composed of dolostone and ooid packstones (GF-e) that materialized the maximum flooding surface. The regressive part (25 m high) is composed of an alternation of grey marls and recrystallized evaporitic mudstones (GF-d). The last 20 m of the sequence are composed of "collapse breccia" by Eichenseer, 1988. The MPU corresponds to the top of this sequence and focused on a boundary between the collapse breccia and red alluvial clays (Da Silva et al., 2009). Above the major sequence boundary, 30 m alluvial and lacustrine to palustrine limestones outcrop. They are ended by a minor subaerial exposure surface, the Colmenar Tremp Horizon (CTH), defined by Eichenseer, 1988.

5.2. Feixa-Rasa section

In the Feixa-Rasa section, the Da2 sequence boundary is a subaerial exposure surface marked by Microcodium biocorrosion. The transgressive part is composed of 7 m of dolomitized ooids packstones. The sea level fall is expressed by more detrital quartz. The maximum of regression is identified by algal mat, surrounded by the MPU, a transition surface between marine limestones and grey-red clay debris.

5.3. Merli section

In the Merli section presented Fig. 4B, the Da2 sequence boundary is an undulating surface that overcomes dolostones affected by syneresis cracks (GF-d). This sequence is 4.5 m thick and is composed of lacustrine to paludal limestones (GF-b to GF-a), with intrusions of miliolids and discocyclines that are evidences of flooding by marine waters in the previous lake. The MPU seems to be set between palustrine limestones and recrystallized porous abiotic limestones which contain detrital quartz.

6. Diagenetic features associated to mid-Paleocene exposure surface

A lot of diagenetic process was identified in the studied sections. In this article, we are focusing only on the description of the subaerial diagenetic features analysed in thin sections. Other phenomena like early shallow burial diagenesis, evaporation diagenesis, cracking, compression, silicification are described by Kiefer-Ollier, 2009.

6.1. Pedogenesis

Description: Pedogenetic features are expressed by root prints filled by green clays, Microcodium bio-corrosion, growing in preexisting cracks of palustrine limestones (GF-a), and preserved paleosoils features like marmorization or rhizocretion (Fig. 3D).

Interpretation: All these features are evidence of an important terrestrial bio-corrosion in epivadose zone or caliche zone located down to 10 cm under the surface. They are associated to periodically flooded subaerial environments like marsh, alluvial soils or flooding plains (Bignot, 1994) under semi-arid to humid climate conditions.

6.2. Epi-karstic dissolutions

Description: In the Campo section, a "brechified" evaporitic limestone 20 m thick underlines the subaerial exposure surface (MPU). It is a polygenic breccia with inframillimetric to centimetric clasts composed of abiotic and evaporitic mudstones, chert, angular dissolved mudstones and lithified red clayey debris (Fig. 3F–G). The debris are covered by a very thin and regular laminar crust, composed of an alternation of micrite and microspar.

Interpretation: This sedimentary system is interpreted as a collapse breccia formed by dissolution of evaporitic minerals and resulting from a delithification inducted by erosive action of meteoric water. Laminar deposits, that rim some clasts, could be due to microbial activity. These two phenomena are evidence of a karstic depression development especially located in Campo area.

6.3. Karstic dissolutions and associated features

Description: Millimetric to centimetric karstic vugs, filled by geopetal carbonated mud, are developed along the subvertical fissuring down to 50 m beneath the MPU (Fig. 3H–L). Caves and cracks located on the collapse breccia are filled by stratified and lithified red and ochre clays. The bottom of the carbonate formation is marked by centimetric or decimetric subhorizontal caves filled by green clayey-dolomites sediments in the Campo section and by an alternation of clayey-mud and partially recrystallised stalactitic concretions (Fig. 3L). The sediments that fill karstic caves down to 30 m beneath the MPU are eroded (Fig. 3). In the Campo section only, the carbonate formation is affected by a corrosion creating "swisscheese" karstic morphology (Fig. 3I–J) and described by Baceta et al., 2007 near Pamplona at the same time.

Interpretation: The caves located along cracks are evidences of paleovertical meteoric water flows from paleosurface to subhorizontal caves, 50 m beneath. Esteban and Wilson, in press describe this process in low-vadose area. The precipitation of concretions is an evidence of calcitic meteoric water percolation.

6.4. Calcitic cementations

Description: The collapse breccia is cemented by a non-luminescent drusy mosaic calcite. In the Merli section, karstic vugs located on the top of the Danian formation are filled by microspar calcite. A part of this cement is eroded and the erosion boundary contains an unusual accumulation of ferric globules. From Campo to Merli, dogtooth or circumgranular (Moore, 2001) calcite crystallizes in vugs created during the last karstic dissolution stage (Fig. 3) down to 30 m beneath the MPU. Luminescence alternations observed in these crystals (Fig. 3La–b) show 7 stages

of crystalline growth with different mineralogical compositions. In the whole Danian carbonates, the last voids are filled by luminescent and slightly magnesian poecilitic calcite (Fig. 3La).

Interpretation: Non-luminescent drusy mosaic calcitic cements contained in the collapse breccia and in Merli caves are interpreted like meteoric phreatic cements due to the formation of a lake system in surface. The interpretation of the diagenetic origin of dogtooth or circumgranular cements that precipitates in Merli section is based on Tucker and Wright, 1990 studies. The luminescence alternations recorded in cements are evidence of marine and freshwater fluctuations. This phenomenon happens certainly in a marine vadose environment. The last luminescent and slightly magnesian poecilitic calcitic cementation indicates a low burial and saturated zone.

6.5. Late dolomitic cementations

Description: In the Campo section, the carbonate formation has been dolomitized from 20 to 80 m under the MPU. The carbonate sediments located at the bottom of the Danian formation are totally recrystallized by an unimodal (20 μm) planar subhedral (Gregg and Sibley, 1984; Sibley and Gregg, 1987) dolomite (D1) characterized by a high Mg/Ca ratio (0.94). The cracks and vugs are cemented by a limpid unimodal (100 μm) planar euhedral dolomite (D2) characterized by a relatively low Mg/Ca ratio (0.76). These dolomites are arranged in idiotopic mosaic and fill corroded "swiss-cheese" caves (Fig. 3I–J). The intercrystalline porous system is filled by clays. The last dolomitic cements (D3) are dirty heart rhombs of 500 μm and characterized by a medium Mg/Ca ratio (0.85).

Interpretation: Based on Warren, 2000 studies, D1 dolomitic cements are interpreted like syndepositional lacustrine "Coorong style" that are associated to a relatively high nucleation rate in evaporate dominated environment. The precipitation of the D2 and D3 dolomites crystals is associated to a shallow burial environment in mixed area under humid climatic conditions. Crystals precipitations associated to karstic corrosions are explained by a tidal influence (Baceta et al., 2007).

6.6. Dedolomitization

Some dolomite crystals are calcified and show the same mineralogical composition as the poecilitic calcite (Fig. 3K). In general, the interpretation of dedolomitization phenomenon in terms of diagenetic environment is relatively complex because of the high extension of the phenomenon. Purser, 1980 indicates examples of a dedolomitization front following a dolomitization stage in a littoral plain. Dedolomitization observed in the Campo section could be due to the same process or to a retroactive phenomenon during the burying.

7. Paleohydrological model associated to the MPU

The crosschecking between each diagenetic process identified in Campo and Merli sections allows us to propose a chronological arrangement of these features and to define a referential diagenetic sequence associated to the MPU in each section. Fig. 5 shows six main diagenetical stages whose petrographical expressions are different according to the environmental and hydrological conditions. The interpretation of diagenetic environments in the south-eastern Pyrenean platform is based on Moore model (Moore, 2001). The sequence took place after marine retirement during the early Lowstand Systems Tract of the Th-1 sequence. Stage 1 is related to syndiagenetic processes such as the gypsum pseumorphism, whose morphology was relatively well preserved. This mechanism of substitution often happened during a shallow burying stage in association with pedogenesis under humid conditions. In the Merli section, the preexistant fissuring of the substratum before Microcodium biocorrosion proves that pedogenesis occurred after a burying stage. The dissolution/recrystallisation process developed in the contact between the Microcodium colonies and substratum is related to pedologic alteration under seasonal climate with alternation of dry and humid conditions (Bignot, 1995). The diagenetic features observed during stages 2 to 4 correspond to the epidiagenesis in the meteoric realm. Stage 2 corresponds to a surface delithification induced by meteoric water infiltration and pedogenesis. In surface, a collapse breccia is created. The vertical infiltration of freshwater in vadose zone is made easier by preexisting cracks (Esteban and Klappa, 1983) and contributes to the karstification of the Danian Formation, recorded down to 60 m under the surface. Diagenetic features of the stage 3 are recorded in the caves previously created. They are geopetal internal sediments and vadose to phreatic cements that show an evolution of the hydrogeological conditions from vadose to phreatic. This event is related to environmental change in paleosurface, particularly well preserved in the Campo section. The Mid-Paleocene Unconformity is surmounted by terrigenous deposits of Lowstand Systems Tract composed of alluvial clayey sediments reddish to greyish, relatively to a negative gradient of oxidation conditions. Upwards, a "stratocroissante" lacustrine sedimentary succession is deposited (see the bottom of "CTH" in Fig. 3). This sedimentary evolution proves that water section increases until a fresh water lake is formed. It could be due to a relative rising of ground water, induced by precipitations or by a local subsidence in continental area. During the stage 4, the deposition of paludal limestones and the Microcodium bio-corrosion show that the lake is progressively drained until subaerial exposure occurs. Down to 50 m beneath this surface, a second karstification stage, that affects ancient caves, is recorded. At the same time, the "swiss-cheese" karst, recorded in the Campo section, results from the mixing-corrosion (Baceta et al., 2001). Stage 5 is marked by the development of several generations of dolomite cements characterizing the mixed zone. The last phreatic calcitic cements analyzed with cathodoluminescence show mineralogical variations during their growth, according to chemical water changes. According to data obtained by Baceta et al., 2007 in the western part of the Pyrenean platform, these cements represent a record of the Thanetian transgression. This

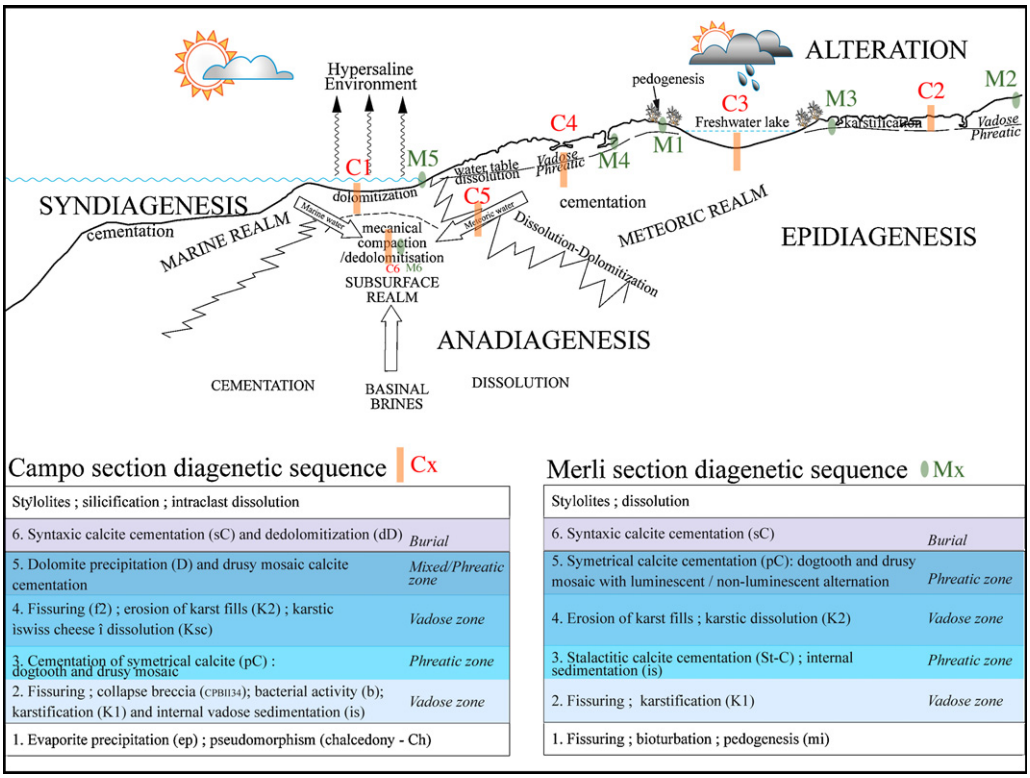

Campo section diagenetic sequence | Cx

Stylolites ; silicification ; intraclast dissolution	
6. Syntaxic calcite cementation (sC) and dedolomitization (dD)	*Burial*
5. Dolomite precipitation (D) and drusy mosaic calcite cementation	*Mixed/Phreatic zone*
4. Fissuring (f2) ; erosion of karst fills (K2) ; karstic iswiss cheese î dissolution (Ksc)	*Vadose zone*
3. Cementation of symetrical calcite (pC) : dogtooth and drusy mosaic	*Phreatic zone*
2. Fissuring ; collapse breccia (CPBI134); bacterial activity (b); karstification (K1) and internal vadose sedimentation (is)	*Vadose zone*
1. Evaporite precipitation (ep) ; pseudomorphism (chalcedony - Ch)	

Merli section diagenetic sequence | Mx

Stylolites ; dissolution	
6. Syntaxic calcite cementation (sC)	*Burial*
5. Symetrical calcite cementation (pC): dogtooth and drusy mosaic with luminescent / non-luminescent alternation	*Phreatic zone*
4. Erosion of karst fills ; karstic dissolution (K2)	*Vadose zone*
3. Stalactitic calcite cementation (St-C) ; internal sedimentation (is)	*Phreatic zone*
2. Fissuring ; karstification (K1)	*Vadose zone*
1. Fissuring ; bioturbation ; pedogenesis (mi)	

Fig. 5. Simplified model of the main diagenetic realms repartition in an emerged platform submitted to a semi-arid to humid climate, inspired of Moore model (Moore, 2001). The chronological sequence of the diagenetic features identified in thin sections is presented of each section. The relative chronology was obtained with a petrographical analysis of the cross-cheking of each diagenetic features.

Fig. 5. Modèle simplifié de la répartition des domaines diagénétiques dans une plate-forme émergée, soumise à un climat semi-aride à humide, d'après Moore (Moore, 2001). Les séquences chronologiques des processus diagénétiques identifiés en lame mince sont présentées pour la coupe de Campo et de Merli. Les chronologies relatives ont été obtenues par identification des recoupements entre les différents caractères diagénétiques.

stage defines the epidiagenesis in a mixed zone. Finally, the stage 6 is related to the last syntaxic calcitic cement and the dedolomitization. This stage belongs to the anadiagenesis.

8. Conclusion

The major sea level fall recorded during the Highstand Systems Tract of the Da-2 sequence in the sections of Campo and Merli is expressed by a depositional environments transition from enclosed marine to hypersaline and littoral systems. The studies of sedimentary and early diagenetic processes allow us to define a paleographic conceptual model based on a hypersaline lagoon and a prograding subtidal sabkha analogous model. The Mid-Paleocene Unconformity is the sequence boundary located between the Da-2/HST and Th-1/LST. It is a subaerial exposure surface that has recorded six main diagenetic events. The first stages are dominated by diagenetic process of meteoric zone influenced by phreatic level fluctuations, recorded 60 m down to the sequence boundary. During the lowstand period, the paleohydrological model is different of the one, dominated by tidal phenomenon, identified by Baceta et al., 2001 in the western part of the platform. This study shows the regional importance of the sea level fall magnitude and its impact on the subjacent limestones. Some similar events were recorded elsewhere in the world during the Middle Paleocene: Clemmensen and Thomsen, 2005; Steurbaut and Sztrákos, 2008 point out an important sea level fall during the Danian/Selandian transition in the North Sea Basin, Ellwood et al., 2008 report the same phenomenon recorded in the southern Tethys. During the Middle Paleocene, Zachos et al., 2001 report a temporary temperature decrease during a global climatic rise until the PETM. Finally, new studies will allow us to determine the effect of local (palegeography), regional (tectonic) and global (climatic) parameters on the sea level fall and particularly the subaerial exposure of the mid-Paleocene.

References

Aguirre, J., Baceta, J.I., Braga, J., 2007. Recovery of marine primary producers after the Cretaceous–Tertiary mass extinction: Paleocene calcareous red algae from the Iberian Peninsula. Palaeogeogr. Palaeoclimatol. Palaeoecol. 249 (3–4), 393–411.

Ardèvol, L., Klimowitz, J., Malagón, J., Nagtegaal, P.J.C., 2000. Depositional Sequence Response to Foreland Deformation in the Upper Cretaceous of the southern Pyrenees, Spain. AAPG Bull. 84 (4), 566–587.

Baceta, J.I., Pujalte, V., Bernaola, G., 2005. Paleocene coralgal reefs of the western Pyrenean basin, northern Spain: New evidence supporting an Earliest Paleogene recovery of reefal ecosystems. Palaeogeogr. Palaeoclimatol. Palaeoecol. 224 (1–3), 117–143.

Baceta, J.I., Pujalte, V., Serra-Kiel, J., Robador, A., Orue-Etxebarria, X., 2004. El Maastrichtiense final, Paleoceno e Ilerdiense inferior de la Cordillera Pirenaica. Geologia de España 308–313.

Baceta, J.I., Wright, V.P., Beavington-Penney, S.J., Pujalte, V., 2007. Palaeohydrogeological control of palaeokarst macro-porosity genesis during a major sea-level lowstand: Danian of the Urbasa–Andia plateau, Navarra, North Spain. Sediment. Geol. 199 (3–4), 141–169.

Baceta, J.I., Wright, V.P., Pujalte, V., 2001. Palaeo-mixing zone karst features from Palaeocene carbonates of north Spain: criteria for recognizing a potentially widespread but rarely documented diagenetic system. Sediment. Geol. 139 (3–4), 205–216.

Bernaola G., 2002. Los nannofósiles calcáreos del Paleoceno en el dominio Pirenaico. Bioestratigrafía, cronoestratigrafía y paleoecología, PhD thesis, Univ. País Vasco, Bilbao.

Bignot, G., 1994. L'énigme des Microcodium. Bull. Soc. Geol. Normandie Havre 81 (2), 25–45.

Bignot, G., 1995. Les deux épisodes à Microcodium du Paléogène parisien replacés dans un contexte péri-téthysien. Newsl. Stratigraphy 32 (2), 79–89.

Casas, A.M., Soto, R., Martínez-Peña, B., 2002. Geometrical relationships between unconformities and subsequent folding: the Arro fold system (southern Pyrenees). C. R. Geoscience 334, 765–772.

Choquette, P.W., Pray, L.C., 1970. Geologic nomenclature and classification of porosity in sedimentary carbonates. AAPG Bull. 54, 207–244.

Clemmensen, A., Thomsen, E., 2005. Palaeoenvironmental changes across the Danian–Selandian boundary in the North Sea Basin. Palaeogeogr. Palaeoclimatol. Palaeoecol. 219 (3–4), 351–394.

Da Silva, A.-C., Loisy, C., Cerepi, A., Toullec, R., Kiefer, E., Humbert, L., Razin, P., 2009. Variations in stratigraphic and reservoir properties adjacent to the Mid-Paleocene sequence boundary, Campo section, Pyrénées, Spain. Sediment. Geol. 219 (1–4), 237–251.

Dinarès-Turell, J., Baceta, J.I., Pujalte, V., Orue-Etxebarria, X., Bernaola, G., 2002. Magnetostratigraphic and cyclostratigraphic calibration of a prospective Paleocene-Eocene stratotypes at Zumaia (Basque Basin, northern Spain). Terra Nova 14, 371–378.

Dinarès-Turell, J., Baceta, J.I., Pujalte, V., Orue-Etxebarria, X., Bernaola, G., Lorito, S., 2003. Untangling the Palaeocene climatic rhythm: an astronomically calibrated Early Paleocene magnetostratigraphy and biostratigraphy at Zumaia (Basque basin, northern Spain). Earth Planet. Sci. Lett. 216, 483–500.

Dunham, R.J., 1962. Classification of carbonate rocks according to depositional texture. In: Ham, W.E. (Ed.), Classification of carbonate rocks. AAPG Memoir, pp. 108–121.

ECORS-team, Choukroune P.,1989. The ECORS Pyrenean deep seismic profile reflexion data and the overall structure of an orogenic belt. Tectonics 8(1), 23–39.

Eichenseer H., 1988. Facies geology of Late Maestrichtian to Early Eocene coastal and shallow marine sediments (Tremp-Graus Basin, northern Spain). PhD thesis, University of Tübingen.

Ellwood, B.B., Tomkin, J., Febo, L., Stuart Jr., C., 2008. Time series analysis of magnetic susceptibility variations in deep marine sedimentary rocks: A test using the upper Danian–Lower Selandian proposed GSSP, Spain. Palaegeogra. Palaeoclimatol. Palaeoecol. 261, 270–279.

Esteban, M., Klappa, C.F., 1983. Subaerial exposure environment. In: Scholle, P.A., Bedout, D.G., Moore, C.H. (Eds.), Carbonate depositional environments: Tulsa, OK, 33. AAPG Memoir, pp. 1–54.

Esteban M., Wilson J. 1993. Introduction to karst systems and paleokarst reservoirs. In: Fritz R. D., Wilson J. L., Yurewicz D. A. (Eds.), Paleokarst-Related Hydrocarbon Reservoirs: Tulsa, 18, SEPM Core Workshop, New Orleans, pp. 1–19.

Flügel, E., 2004. Microfacies of Carbonate Rocks, Analysis, Interpretation and Application. Springer-Verlag, Berlin, Heidelberg, New York, 976 p.

Gregg, J., Sibley, D., 1984. Epigenetic dolomitization and the origin of xenotopic dolomite texture. J. Sedimentary Res. 54, 908–931.

Kiefer-Ollier E., 2009. Caractérisations sédimentaire et diagénétique des surfaces d'émersion, propriétés réservoirs associées. Exemple de la plate-forme carbonatée sud-pyrénéenne au Paléocène moyen. PhD thesis, Université de Bordeaux 3.

Lindsay R. F.: Madison Group (Mississippian) Reservoir Facies of Williston Basin, North Dakota. AAPG Bull., v. 69.

López-Martínez N., Dinarès-Turrell J., Elez-Villar J.: Chronostratigraphy of the continental Paleocene series from the South Central Pyrenees (Spain): new magnetostratigraphic constraints. CBEP International Meeting, Abstract volume, Bilbao, Spain.

Lucia, F.J., 1995. Rock-fabric/petrophysical classification of carbonate pore space for reservoir characterization. AAPG Bull. 79, 1275–1300.

Martini, E. 1970. Standard Tertiary and Quaternary calcareous nannoplankton zonation. In: Farinacci, A. (Ed.), Proc. 2nd Int. Conf. Planktonic Microfossils: Roma, v. 2, pp. 739–785.

McClay, K., Muñoz, J., García-Senz, J., 2004. Extensional salt tectonics in a contractional orogen: A newly identified tectonic event in the Spanish Pyrenees. Geology 32 (9), 737–740.

Moore, C.H., 2001. Carbonate reservoirs porosity evolution and diagenesis in a sequence stratigraphic framework. Developments in sedimentology, 55. Elsevier.

Muñoz J. A., 1992. Evolution of continental collision belt: ECORS-Pyrénées central balanced cross-section. K. Clay (Ed.), Thrust tectonics, pp. 232–246.

Orue-Etxebarria, X., Pujalte, V., Bernaola, G., Apellaniz, E., Baceta, J.I., Payros, A., Nuñezbetelu, K., Serra-Kiel, J., Tosquella, J., 2001. Did the Late Paleocene thermal maximum affect the evolution of larger foraminifers? Evidence from calcareous plankton of the Campo Section (Pyrenees, Spain). Marine Micropaleontol. 41 (1–2), 45–71.

Payros, A., Pujalte, V., Orue-Etxebarria, X., 1999. The South Pyrenean Eocene carbonate megabreccias revisited: new interpretation based on evidence from the Pamplona Basin. Sediment. Geol. 125 (3–4), 165–194.

Plaziat J., 1984. Le domaine pyrénéen de la fin du Crétacé à la fin de l'Éocène : stratigraphie, paléoenvironnement et évolution paléogéographique, PhD thesis, Université de Paris-Sud, 3 tomes.

Pujalte, V., Baceta, J.I., Dinarès-Turell, J., Orue-Etxebarria, X., Parès, J., Payros, A., 1995. Biostratigraphic and magnetostratigraphic intercalibration of Latest Cretaceous and Paleocene depositional sequences from the deep-water Basque basin, western Pyrénées, Spain. Earth Planet. Sci. Lett. 136, 17–30.

Pujalte, V., Baceta, J., Payros, A., Robador, A., 2006. General introduction. In: Baceta, J.I., Pujalte, V., Caballero, F. (Eds.), Palaeocene and Early Eocene Facies and Events: a Basin-Platform-Coastal Plain Transect (South-central and Western Pyrenees). Climate and Biota of the Early Paleogene 2006. Post Conference Field Trip Guidebook, Bilbao, pp. 1–10.

Pujalte V., Orue-Etxebarria X., Schmitz B., Tosquella J., Baceta J. I., Payros A., Bernaola G., Caballero F., Apellaniz E., 2003. Basal Ilerdian turnover of larger foraminifera: Age constraints based on calcareous plankton and $\delta^{13}C$ isotopic profile from new southern Pyrenean sections (Spain). In: Wing S. L., Gingerich P. D., Schmitz B., Thomas E. (Eds.), Causes and Consequences of Globally Warm Climates in the Early Paleogene, The Geological Society of America Special Paper, v. 369, pp. 205–221.

Purser, B.H., 1980. Sédimentation et diagenèse des carbonates néritiques récents. Technip 1 366 p.

Robador A., 2005. El Paleoceno e Ilerdiense inferior del Pireneo occidental: Estratigrafía y Sedimentología. PhD thesis, Universidad País Vasco.

Schmitz, B., Pujalte, V., 2003. Sea-level, humidity, and land-erosion records across the initial Eocene thermal maximum from a continental-marine transect in northern Spain. Geology 31 (8), 689–692.

Sibley, D.F., Gregg, J.M., 1987. Classification of dolomite rock textures. J. Sedimentary Petrology 57, 967–975.

Steurbaut, E., Sztrákos, K., 2008. Danian/Selandian boundary criteria and North Sea Basin–Tethys correlations based on calcareous nannofossil and foraminiferal trends in SW France. Marine Micropaleontol. 67 (1–2), 1–29.

Toullec R., 2006. Genèse et diagenèse des plates-formes carbonatées Paléogène et Crétacé supérieur du Sud du Bassin Aquitain. Contrôles sédimentaires et diagénétiques de leurs propriétés réservoirs. PhD thesis, université de Bordeaux 3.

Tucker, M.E., Wright, V.P., 1990. Carbonate sedimentology. Blackwell 482.

Vail, P.R., Mitchum, R.M., Thompson, S., 1977. Seismic stratigraphy and global changes of sea level; Part 4: global cycles of relative changes of sea level. Seismic stratigraphy, 26. AAPG Memoir, pp. 83-97.

Warren, J., 2000. Dolomite: occurrence, evolution and economically important associations. Earth-Science Rev. 52 (1–3), 1–81.

Zachos, J., Pagani, M., Sloan, L., Thomas, E., Billups, K., 2001. Trends, Rhythms, and Abberrations in Global Climate 65 Ma to Present. Science 292, 686–693.